International Journal of Pharmaceutics 644 (2023) 123318

Contents lists available at ScienceDirect

International Journal of Pharmaceutics

journal homepage: www.elsevier.com/locate/ijpharm

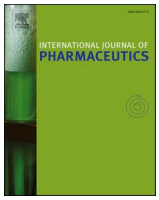

Wet granulation of co-amorphous indomethacin systems

David Schütz, Annika Timmerhaus, Holger Grohganz *

Department of Pharmacy, University of Copenhagen, Copenhagen, Denmark

ARTICLE INFO

Keywords:
Amino acid
Co-amorphous
Downstream processing
Molecular interactions
Solid state
Wet granulation

ABSTRACT

The feasibility of co-amorphous systems to be wet granulated together with microcrystalline cellulose (MCC) was investigated. Solid state and molecular interactions were analysed for various co-amorphous drug-amino acid formulations of indomethacin with tryptophan and arginine, respectively, via XRPD, DSC and FTIR. The co-amorphous binary systems were produced by ball-milling for 90 min at different molar ratios followed by wet granulation with MCC and water in a miniaturised scale. Tryptophan containing systems showed crystalline reflections in their XRPD diffractograms and endothermal events in their DSC analyses, and were therefore excluded from upscaling attempts. The systems containing arginine were found to be remain amorphous for at least ten months and were upscaled for production in a high-shear blender under application of two different parameter settings. Under the harsher instrument settings, a composition with a low MCC ratio experienced recrystallisation during wet granulation, while all other compositions could be successfully processed via wet granulation and stayed stable for a storage period of at least twelve weeks, indicating that wet granulation of co-amorphous systems can be feasible.

1. Introduction

Many present-day drug candidates exhibit poor water solubility (Hauss, 2007) which can reduce the oral bioavailability of these active pharmaceutical ingredients (APIs) (Di et al., 2012; Khadka et al., 2014). Amorphous forms of these drug candidates show promising properties in terms of solubility and oral bioavailability (Zhang et al., 2020). Amorphous systems do not possess long-range crystallographic order and experience a bulk relaxation (Ke et al., 2012) that leads to a higher energy level compared to the crystalline systems of the respective drug (Korhonen et al., 2016). The higher energetic level can not only cause a higher apparent solubility but also an increased dissolution rate (Fael & Demirel, 2021). On the other hand, due to this higher energy level, amorphous systems are less stable than the respective crystalline drug and tend to recrystallize to regain a more stable state of lower energy (Cruz-Angeles et al., 2019; Liu et al., 2021b). This problem could be overcome using i.e., solid dispersions which can be used to stabilize the amorphous form of the drug (Vasconcelos et al., 2007).

Co-amorphous systems (CAMs) are another promising approach to overcome this limitation (Grohganz et al., 2013). In a CAM, at least two initially crystalline compounds form a homogenous amorphous mixture after processing (Han et al., 2020; Liu et al., 2021a). All components are characterised by a low molecular weight (Guinet et al., 2023). These systems can contain compounds that per se are almost impossible to form stable amorphous systems i.e., carbamazepine (Ambrogi et al., 2013; Fael & Demirel, 2020), The stabilizing effects within the CAM are caused by interactions between the API(s) and the co-former(s), such as π-π stacking, hydrogen bonds or salt formation (Karagianni et al., 2018; Löbmann et al., 2013b). Stable CAMs could be achieved with for example drug-drug (Löbmann et al., 2012), drug-organic acid (Fung et al., 2018; Hoppu et al., 2007), and drug-amino acid compositions (Hatwar et al., 2021; Löbmann et al., 2013a).

A high glass transition temperature (T_g) is usually seen as a marker for stability: the higher the T_g, the higher the energetic barrier that needs to be overcome before recrystallization takes place. This leads to a stabilization of the CAM compared to the respective mono-compound amorphous drug system since CAMs often show a higher T_g than the pure amorphous drug (Jensen et al., 2016b).

Indomethacin (Ind) is a model drug that already has been widely used for CAMs with drugs like ranitidine hydrochloride or naproxen and amino acids like L-arginine, L-tryptophane or L-phenylalanine (Ojarinta et al., 2017). Ind is a non-steroid anti-rheumatic drug used for analgetic purposes (Hart & Boardman, 1963) and is classified as a class II drug according to the Biopharmaceutical Classification System (BCS) (Fu et al., 2019). In previous studies it was shown that Ind can form CAMs with the amino acids Arg and Trp via quench cooling (Lim et al., 2016),

* Corresponding author at: Department of Pharmacy, University of Copenhagen, Universitetsparken 2, 2100 København Ø, Denmark.
E-mail address: holger.grohganz@sund.ku.dk (H. Grohganz).

https://doi.org/10.1016/j.ijpharm.2023.123318
Received 13 June 2023; Received in revised form 11 August 2023; Accepted 13 August 2023
Available online 14 August 2023

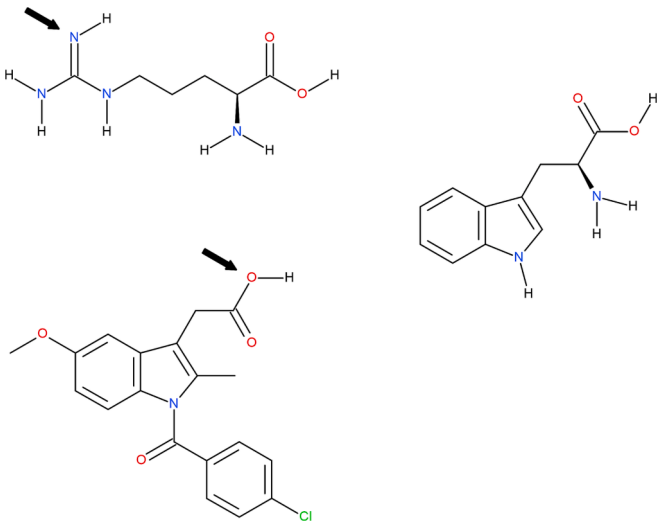

Fig. 1. Chemical structure of Arg (upper left), Ind (lower left) and Trp (right). The arrows indicate where a positive charge (Arg) and a negative charge (Ind) are located when both substances are exposed to aqueous conditions close to pH 7.

spray drying (Lenz et al., 2015) or ball milling (Lenz et al., 2017). Ball milling was mostly used as a preparation method for miniaturised scaled batches (Heikkinen et al., 2015).

Storage stability of CAMs is closely connected to both storage temperature and humidity (Chavan et al., 2016). With an increased water content, recrystallization usually occurs faster due to a decrease of the T_g (Ueda et al., 2018). The molecular interactions within CAMs are weakened by the presence of humidity, which therefore can result in salt disproportionation (for salt forming systems) and consequently lead to recrystallization – generally to a meta-stable form (Surwase et al., 2013). Depending on the moisture content, the optimal molar ratio within a binary co-amorphous system can vary as well as the form to which the co-amorphous system recrystallizes. In addition to that, a high T_g measured right after production is not suitable to predict the physical stability of a system under moist conditions (Liu et al., 2021b). Based on these findings, moisture is one of the main influences that impact the quality of CAMs.

It has been shown that compaction of CAMs is possible without recrystallization, indicating the feasibility of tablets containing CAMs (Ojarinta et al., 2018; Sørensen et al., 2023). However, due to the small size of the co-amorphous particles, which are usually prepared via ball-milling or spray-drying, and their high cohesiveness (da Costa et al., 2022b), flowability can be assumed to be a challenge in further downstream processing. In a previous study, downstream processing of amorphous solid dispersions (ASDs) via wet granulation was investigated (Trasi et al., 2019): an organic dispersion of a polymer and the drugs ritonavir and lopinavir, respectively, was added to a dry excipient mixture followed by the formation of granules through wet granulation. The consecutive analysis included XRPD and FTIR and showed the successful amorphization of the drugs. Additional dissolution testing was performed as well as content analysis with HPLC, whereas no DSC analysis, no storage stability testing and no particle size analysis was executed.

Another attempt was the wet granulation of olanzapine CAMs (da Costa et al., 2022a). In this case, the CAMs were obtained via solvent evaporation with saccharin, and were further processed with calcium hydrogen phosphate, polyvinylpyrrolidone, microcrystalline cellulose (MCC) and water to form granules, extrudates and pellets. The solid state was assessed via XRPD, DSC, FTIR and NIR and dissolution testing was performed. No storage stability testing or particle size analysis was conducted.

In contrast to these studies, it was the aim of the current study to find out whether water as a worst-case granulation liquid for amorphous systems is applicable to CAMs of other drugs than olanzapine. More specific it was the aim to perform a feasibility study of wet granulation of CAMs of Ind with the amino acids L-arginine (Arg) and L-tryptophan (Trp), as a respective salt-forming and non-salt forming co-former, to investigate the influence of molecular interactions on the stability of CAMs. The number and mass ratio of excipients was reduced to increase the drug loading, and MCC as an established excipient for granulation (Saigal et al., 2009) was the only added excipient. Furthermore, the influence of production parameters on the physical stability of the amorphous form was tested by selecting two different settings for blending and granulation. Solid state analysis for the CAMs, as well as for the granules, was performed with XRPD, DSC and FTIR after production and after storage.

Table 1
Mass ratios of each compound in miniaturised granule batches.

Batch	binary co-amorphous system [g]	MCC [g]	Water [ml]
miniaturised MCC 80:20 Ind:Arg 1:1	1.35	5.41	4.9
miniaturised MCC 60:40 Ind:Arg 1:1	2.07	3.11	2.0
miniaturised MCC 80:20 Ind:Arg 1:1.5	1.18	4.71	5.0
miniaturised MCC 60:40 Ind:Arg 1:1.5	2.76	4.14	1.0
miniaturised MCC 80:20 Ind:Trp 1:1	1.54	6.19	4.0
miniaturised MCC 60:40 Ind:Trp 1:1	2.85	4.28	2.5
miniaturised MCC 80:20 Ind:Trp 1:3	1.23	4.93	5.0
miniaturised MCC 60:40 Ind:Trp 1:3	2.06	3.09	2.4

2. Materials and methods

2.1. Material

Indomethacin (Ind) was obtained from Hovione Farmaciencia SA (Loures, Portugal). Tryptophan (Trp) was supplied by EMD Millipore Corporation (Burlington MA, USA) whereas arginine (Arg) was produced by Thermo Fischer Scientific (Kandel, Germany). The chemical structures of all three substances are shown in Fig. 1. The respective pK_a values lie at 13.8 for the guanidine group of Arg (Fitch et al., 2015) and at 4.5 for the carboxylic acid moiety of Ind (O'Brien et al., 1984). The side chain of Trp has no potential for (de)protonation. The transfer or protons between Ind and Arg can lead to salt formation (Ojarinta et al., 2017).

Microcrystalline cellulose (MCC PH-102) was delivered by Roquette Brazil (Itapevi, Brazil). The T_g values of various amorphous systems were reported as follows: the T_g of an equimolar co-amorphous Ind:Arg system at 117.5 (±0.4) °C, the T_g of Ind at 36.70 (±0.8) °C and the T_g of Arg at 55 °C (Jensen et al., 2016a) as well as the T_g value for an equimolar co-amorphous Ind:Trp system at 90 °C (Jensen et al., 2016b).

2.2. Methods

2.2.1. Preparation of co-amorphous systems

Binary co-amorphous systems of different molar ratios were produced with Ind and the respective co-former (1:1 and 1:1.5 for Ind:Arg, 1:1 and 1:3 for Ind:Trp). These systems were obtained by ball milling 750 mg of the respective composition in 25-mL jars with 12-mm balls of stainless steel using an oscillatory ball mill (Mixer Mill MM400, Retsch GmbH, Haan, Germany) for 90 min at a frequency of 30 Hz. The ball mill was constantly cooled down to 6 °C to reduce recrystallization. The

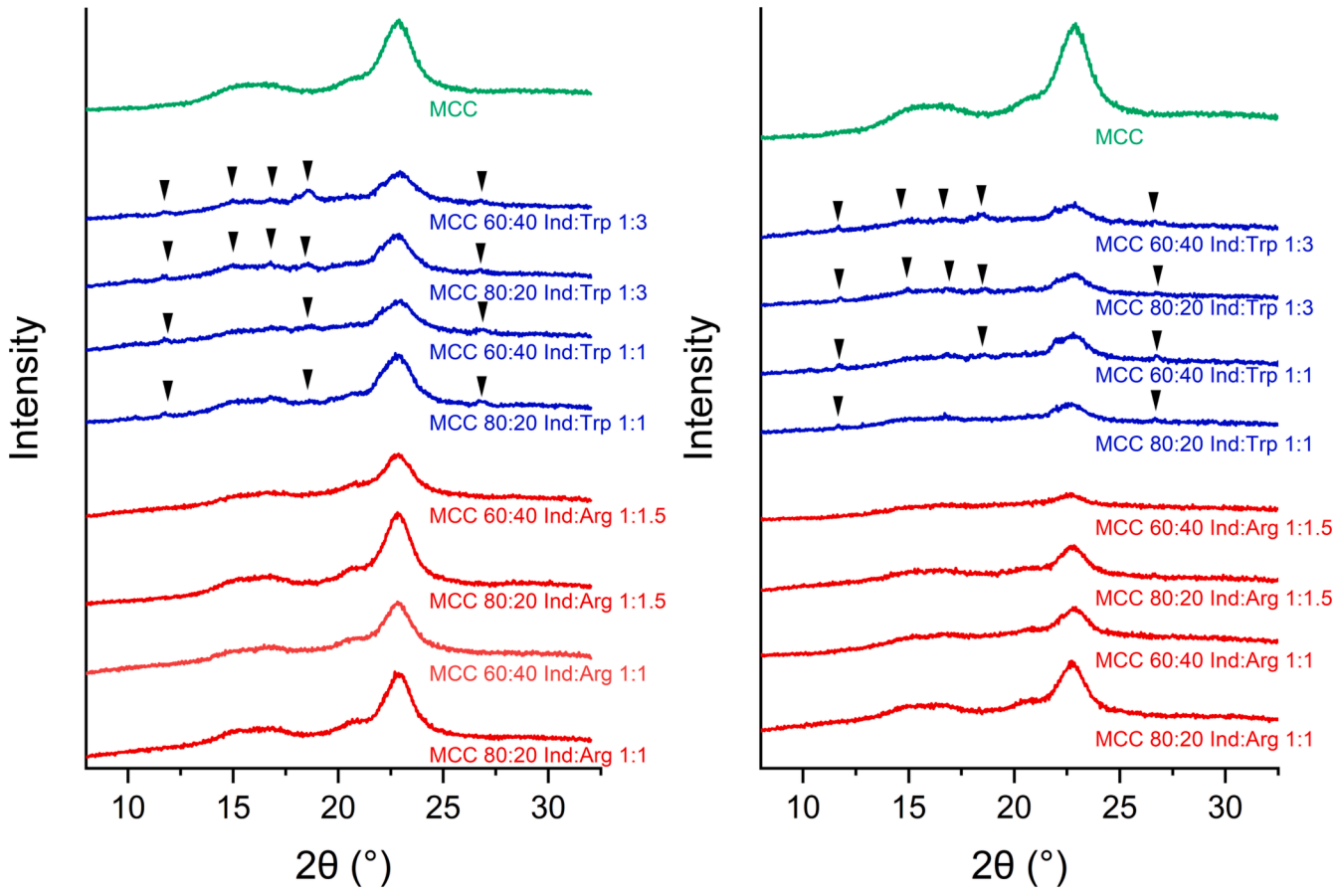

Fig. 2. XRPD diffractograms of miniaturised batches after manufacturing (left) and after a storage period of ten months (right). The arrows indicate deviations from the MCC diffractogram which are interpreted as crystalline reflections originating from Ind and Trp.

success of amorphization was tested with XRPD and DSC before proceeding with granulation.

2.2.2. Granulation process

Due to the limited availability of co-amorphous material, preliminary investigations for wet granulation were performed via a Gefu Aglioli garlic chopper (GEFU GmbH, Eslohe, Germany) as a granulator. Total amounts between 7.5 g and 11.5 g of granules (prior to drying) were produced before a scale-up to lab-scaled batches could take place. First, MCC was added to the binary co-amorphous systems with a mass ratio of 80 % and 60 %, respectively, for each investigated Ind-amino acid molar ratio. The ternary systems were mixed to form a homogenous powder. Using a syringe, water was added dropwise to avoid stressing the system. When the system reached snowball consistency, it was sieved through a 900 µm sieve and dried in an oven at 55 °C for the Ind-Arg compositions and at 35 °C for the Ind-Trp compositions. In total, eight different compositions with varying ratios between drug and co-former, and between the CAM and MCC, were produced in a miniaturised scale (Table 1).

Based on the results from the miniaturised approach, transfer of promising amorphous batches to a laboratory scale high shear blender was conducted. The upscaled batches of Ind:Arg granules were produced in an high shear mixer E150 - TMG 1/6 (Glatt Systemtechnik GmbH, Dresden, Germany). The two conditions for the upscaled production were either setting F (fast) (rotator: 500 rpm, chopper: 1500 rpm, initial mixing: 10 min) or setting S (slow) (rotator: 400 rpm, chopper: 1000 rpm, initial mixing: 2 min). Both settings were applied to MCC 80:20 Ind:Arg 1:1 and MCC 60:40 Ind:Arg 1:1 so that in total four upscaled batches were produced. In each case water was added dropwise with a syringe until snowball consistency was reached. The system was then sieved through a 1000 µm sieve and dried for 3 h at 45 °C.

2.2.3. X-Ray powder diffraction (XRPD)

The granules were measured via XRPD with an X'Pert PRO X-ray Diffractometer (PANalytical B.V., Almelo, Netherlands) using Cu Kα (λ = 1.541874 Å) radiation with an acceleration voltage of 45.0 kV and a current of 40.0 mA. Depending on the instrument either a PIXcel1D RTMS detector with a step size of 0.02606° or an X'Celerator Scientific RTMS detector (both: PANalytical B.V., Almelo, Netherlands) with a step size of 0.03342° was used. All samples were measured in reflection mode from of 5° to 35° 2θ. For data collection and analysis, X'Pert Data Collector Version 7.2b and X'Pert Data Viewer Version 2.2 (both: Panalytical B.V., Almelo, Netherlands) were applied.

2.2.4. Differential scanning calorimetry (DSC)

The used instrument was a Q2000 DSC-97001.901 (TA Instruments Inc., New Castle DE, USA), the nitrogen flow was set to 50 mL/min. Samples were measured in hermetic aluminium pans with pin-holed lids to enable absorbed water to escape the sample during heating. The selected method consisted of sample equilibration at 10 °C, keeping this temperature isothermal for 2 min before ramping with 2 °C/min up to 180 °C using a modulation of ± 0.212 °C every 40 s. With this modulation a reversed sample heat flow could be calculated, using the TRIOS software (TA Instruments Inc., New Castle DE, USA) to determine T_g.

2.2.5. Fourier transformation Infra-Red spectrometry (FTIR)

FTIR spectra were measured right after granule production and compared to the spectra of the single crystalline components. On an FT-IR Laboratory Spectrometer MB3000 (ABB, Zurich, Switzerland) the attenuated total reflection (ATR) accessory MIRacle™ Single reflection

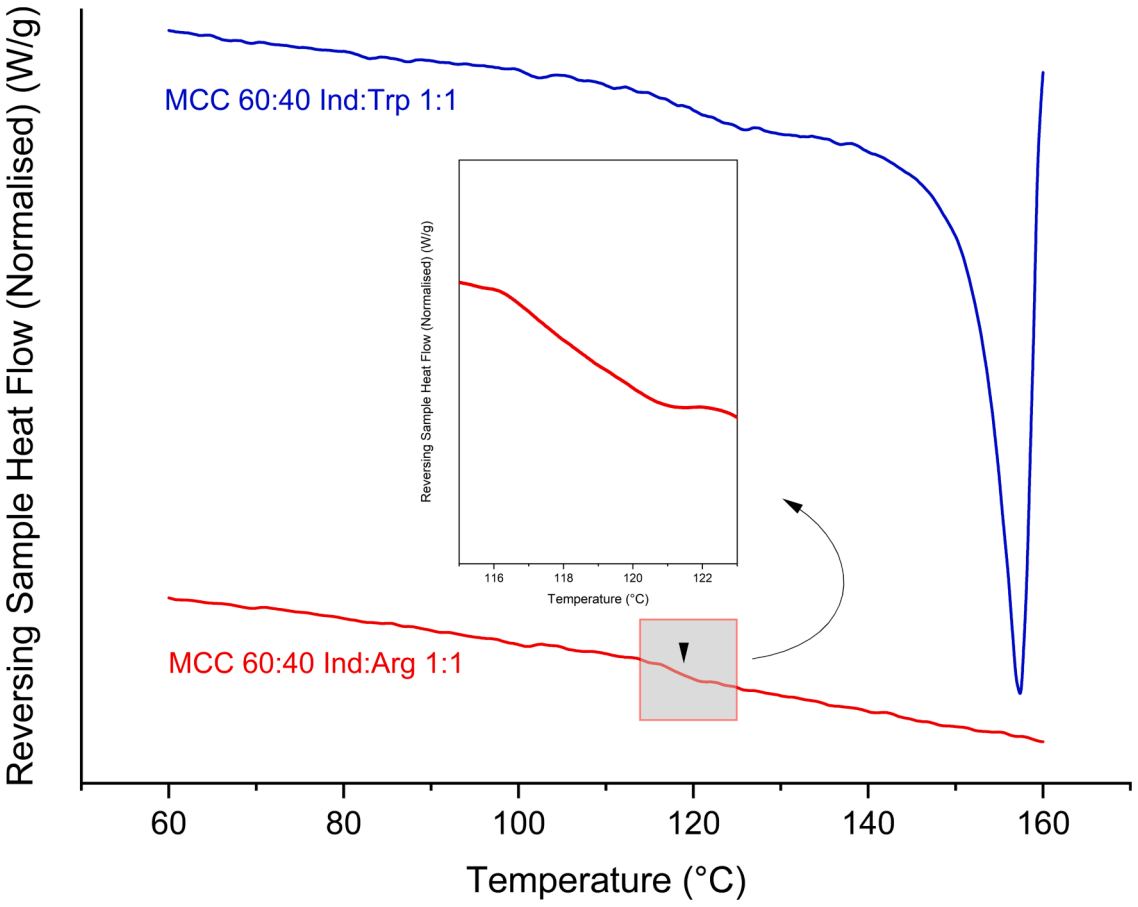

Fig. 3. DSC diagrams of miniaturised MCC 60:40 Ind:Trp 1:1 (top; blue) and miniaturised MCC 60:40 Ind:Arg 1:1 (bottom; red). The straight arrow indicates the the range of temperature where a step change in the reversing sample heat flow is located which is interpreted as T_g of the corresponding sample.

ATR (PIKE Technologies, Fitchburg, WI, USA) was attached. Analyses were performed by Horizon MB™ FTIR software (ABB, Zurich, Switzerland). The spectra were measured as the mean of 64 spectra within the range of 1400 to 1800 cm^{-1} with a resolution of 4 cm^{-1}.

2.2.6. Storage stability

The upscaled samples were stored under dry conditions in a desiccator with silica beads that were previously dried for 180 min at 120 °C. The storage conditions were a temperature around 20 °C and a relative humidity (RH) below 5 %. The samples' stability was analysed via XRPD, DSC and FTIR up to a storage time of at least twelve weeks. The miniaturised batches were stored under the same conditions for a period of ten months.

2.2.7. Granule particle size analysis

The granules' grain size was assessed via the vibrating sieve shaker Analysette 3 (Fritsch GmbH, Idar-Oberstein, Germany). Around 50 g of granule were analysed via a sieving tower with seven laboratory test sieves (Retsch GmbH, Haan, Germany) with sieve sizes of 1000, 710, 500, 355, 250, 125 and 75 µm. Via the remaining granule mass per sieve the passage sum was calculated and entered in a RRSB net. The analysis of the characteristic grain diameter $d_{63.2}$, the uniformity index n and the specific surface index $S_v d'/f$ was performed according to Rosin, Rammler, Sperling and Bennet (RRSB). The characteristic grain diameter $d_{63,2}$ describes the theoretical sieve size at which a passage sum of 63.2 % is reached. The uniformity index n is a parameter to measure the distribution range of particle sizes: the higher the value of n, the higher the uniformity (Tangirala et al., 2014).

3. Results and discussion

Due to the limited availability of co-amorphous material, initial investigations on the feasibility of granulation were conducted on a miniaturised scale. Subsequently, formulations that were successfully granulated without showing recrystallization were transferred to a standard laboratory-scale high shear blender. Preliminary experiments showed that amorphization could not be achieved through high mechanical energy input to pure Ind, and furthermore no co-amorphous granules could be produced by direct wet granulation of the crystalline compounds. Since neither crystalline Ind nor the mixture of crystalline Ind and the respective crystalline amino acid could be amorphized in-situ by using a high share blender, a preceding production of co-amorphous Ind:Arg and Ind:Trp systems was necessary.

3.1. Miniaturised preparation

3.1.1. Production of miniaturised batches

The miniaturised batches were produced as described in chapter 2.2.1 and 2.2.2. The amorphous nature of the secondary systems (Ind:Trp and Ind:Arg) was confirmed by XRPD before the CAM was used to produce granules. The amounts of added material for all miniaturised batches are shown in Table 1. The results were batches of five to eight grams of yellowish granules. The content of added water (until reaching snowball consistency) depended on the amount of MCC in the composition: the higher the MCC ratio, the more water was need to obtain a plastic mass.

3.1.2. Solid state of miniaturised granules

Each of the miniaturised granule samples was tested for successful

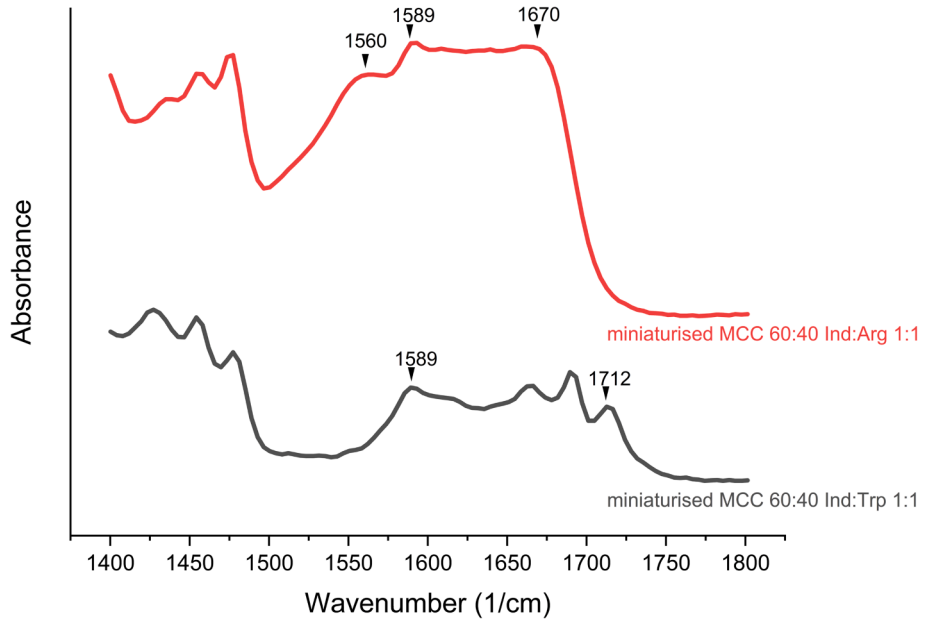

Fig. 4. FTIR spectra of miniaturised MCC 60:40 Ind:Arg 1:1 and miniaturised MCC 60:40 Ind:Trp 1:1. The arrows indicate peaks of each FTIR spectrum that are characteristic for either co-amorphous or crystalline samples.

amorphization via XRPD and DSC. Successful amorphization was indicated by a halo in the XRPD diffractograms without any sharp reflections caused by crystalline components. In Fig. 2 the diffractograms of all eight miniaturised granules are shown after manufacturing (left), as well as after ten months of storage (right). The diffractogram of pure MCC is given as a reference, since MCC is by far each system's largest compound by mass and therefore sets the shape of the expected diffraction pattern. All granules containing Trp (blue graphs) show clear reflections of crystallinity after production. The following trend is recognizable: The higher the molar Trp ratio in the binary co-amorphous Ind:Trp system and the higher the Ind:Trp mass ratio in the granule, the more crystalline reflections are visible. At batch MCC 60:40 Ind:Trp 1:3 the clearest reflections can be detected at 11.8, 15.0, 17.0, 18.5 and 26.8 °2θ. The reflections at 11.8, 17.0 and 26.8 °2θ are attributed to recrystallised γ-Ind whereas the reflections at 15.0 and 18.5 °2θ are attributed to recrystallised Trp.

The diffractograms of the Arg containing granules (red graphs) show an MCC-dominated halo after production (left) without obvious changes over a storage period of ten months (right). Since the diffractograms of the Trp containing granules already showed clear crystallinity reflections right after production, it can be stated that Trp lacks the ability to successfully be processed to co-amorphous granules via wet granulation under the current setup. As the amount of added water to reach a plastic mass depended on the MCC portion and not the type of CAM, the observed recrystallisation of the systems with Trp cannot be explained by unreasonably high amounts of water. It has been shown for co-amorphous powders that the addition of water can lead to a locally higher level of molecular mobility and may enable amorphous-amorphous phase formation and recrystallisation (Liu et al., 2021b). The crystallinity reflections of the formulations with Trp did not intensify during the storage period.

Next to XRPD, all miniaturised samples were analysed via DSC. In Fig. 3, the DSC diagrams of the two compositions miniaturised MCC 60:40 Ind:Arg 1:1 and miniaturised MCC 60:40 Ind:Trp 1:1 – each exemplary for systems with the respective co-former – are shown after four months of storage. The composition containing Arg (bottom; red), did not show any melting event, but a T_g at 118.3 °C (close to the literature value of 117.5 ± 0.4 °C (Lenz et al., 2017)). The composition with Trp (top; blue) did not exhibit a T_g but a clear endothermal event around 158 °C, indicating the presence of crystalline Ind (Surwase et al., 2013). Due to a missing exothermal recrystallisation event in the DSC diagram the recrystallisation must have taken place during granulation. The T_g of equimolar Ind:Trp systems at 90 °C cannot be observed. These results, measured after four months, correspond well with the freshly prepared samples. The Trp containing systems could not retain their amorphous nature upon wet granulation.

Summarising, neither XRPD nor DSC analysis gave any indication for recrystallisation of the Ind:Arg systems upon granulation or storage. In contrast, indications for the recrystallisation of both Trp (XRPD) and Ind (XRPD and DSC) were given for the Ind:Trp systems.

3.1.3. Molecular interaction properties

It has been reported that Ind:Arg systems form a co-amorphous salt, while no strong interaction was found for Ind:Trp (Ojarinta et al., 2017). It was thus of importance to see if the existing bonding pattern could be retained throughout granulation. The FTIR spectra of miniaturised MCC 60:40 Ind:Arg 1:1 and miniaturised MCC 60:40 Ind:Trp 1:1 are shown in Fig. 4 as representatives for the miniaturised systems with both co-formers.

The spectrum of miniaturised MCC 60:40 Ind:Trp 1:1 shows a peak at 1712 cm^{-1} which is caused by the stretching vibration of a carboxylic acid moiety (Gershevitz & Sukenik, 2004). Since this moiety is the functional group with the lowest pK_a value in the structure of Ind (O'Neil, 2013) and is still protonated, no salt formation had taken place. Next to the band at 1712 cm^{-1} another less distinct peak is shown at 1589 cm^{-1} which can be found in all systems containing Ind.

Unlike these Trp containing systems, the granules with Arg showed a plateau from 1589 to 1670 cm^{-1} and a sharp drop of absorbance from 1670 to 1735 cm^{-1} which is in accordance with prior studies and attributed to the salt formation between Ind and Arg (Lenz et al., 2017). The spectrum of miniaturised MCC 60:40 Ind:Arg 1:1 clearly shows no peak around 1700 cm^{-1} indicating that the carboxylic acid moiety of Ind is deprotonated. A hardly distinct band that forms a clearly visible upstream shoulder is shown at 1560 cm^{-1} (its absorbance starts at a wavelength of 1500 cm^{-1}), next to the plateau which can only be found in the systems containing Arg. This feature is caused by the corresponding carboxylate stretching vibration of Ind (Jensen et al., 2016a). The salt forming partner in these granules is the co-former Arg that experiences a protonation. The final granules show comparable spectra to their respective binary drug–co-former system (see Figure S1 for the

Table 2
Mass ratio of each compound in upscaled granule batches and their grain characteristics.

System	co-amorphous Ind-Arg [g]	MCC [g]	Water [ml]	$d_{63.2}$ [µm]	N	$S_v d'/f$
MCC 80:20 Ind:Arg 1:1 F	16.6	67.0	18.5	~650	~2.50	~8.6
MCC 80:20 Ind:Arg 1:1 S	16.9	67.1	16.0	~490	~2.15	~9.4
MCC 60:40 Ind:Arg 1:1 F	33.7	50.5	17.0	~525	~1.82	~11.0
MCC 60:40 Ind:Arg 1:1 S	33.5	50.3	12.0	~500	~2.50	~8.5

co-amorphous and crystalline IND-ARG physical mixture with MCC). It can be concluded for the miniaturised batches that the Ind:Arg systems are able to retain their salt form upon wet granulation with MCC and water. The Trp containing systems cannot be wet granulated without recrystallizing, presumably because of their weak molecular interactions. Only the co-amorphous systems containing Arg were considered for further downstream processing.

Out of the four systems with Arg previously produced and analysed, the two compositions with a 1:1 M ratio of Ind:Arg were selected for downstream processing since the modified Gordon-Taylor Equation showed the highest deviation from the theoretical T_g at this molar ratio (Jensen et al., 2016b) with a T_g between 112 °C and 120 °C.

3.2. Upscaled preparation

3.2.1. Characterisation of particulate properties

In order to account for the different energy input in the laboratory scale high-shear blender, two different process settings (fast setting F and slow setting S, as described in chapter 2.2.2.) were investigated to elucidate whether time and granulation speed are of importance. The amounts of added material for all upscaled batches are shown in Table 2. The granules were assessed with a vibrating sieve shaker and showed comparable particulate properties: the characteristic grain diameter $d_{63.2}$ varies between roughly 490 and 620 µm, the uniformity indices n are identified as approximately 1.8 to 2.5 and the surface indices $S_v d'/f$ as approximately 8.5 to 11 (Table 2).

3.2.2. Solid state and molecular interactions of upscaled batches

Granules were tested for successful amorphization via XRPD and DSC, while molecular interactions were determined via FTIR. The XRPD diffractograms after production are shown in Fig. 5 (left). MCC 60:40 Ind:Arg 1:1 F (red graph) shows crystalline reflections at 13.4, 14.2, 14.7, 15.1, 17.7, 19.0, 20.4, 21.0, 21.5, 24.2, 25.0, 26.0 and 29.3 °2θ whilst the other three batches show an MCC-like halo and therefore can be judged as XRPD-amorphous. The crystalline reflections of MCC 60:40 Ind:Arg 1:1 F were compared to diffractograms of polymorphs of Ind. It can be concluded that the reflections are most likely caused by α-Ind. Amorphous Ind usually recrystallizes to metastable α-Ind or thermodynamically stable γ-Ind. The recrystallization to the α-form is enhanced by high humidities and temperatures that are near or above the respective co-amorphous system's T_g (Surwase et al., 2013). Since the high-shear blender was not cooled and due to the addition of water to the batch MCC 60:40 Ind:Arg 1:1 F (Table 2), the conditions favouring recrystallization into the α-form were met during granulation. No reflections of recrystallised Arg could be found which either indicates that the co-amorphous phase is over-proportionally rich of Arg or a lower sensitivity of the applied XRPD method towards Arg reflections.

Of the amorphous samples, the DSC diagrams of MCC 80:20 Ind:Arg 1:1 S and MCC 60:40 Ind:Arg 1:1 S exhibited T_gs around 117 °C. No endo- or exothermal events were found (Figure S2). The DSC of MCC 80:20 Ind:Arg 1:1 F showed neither a clear T_g nor endo- or exothermal events, which indicates that the sample is co-amorphous, but its T_g signal is too weak to be clearly detectable due to the high ratio of MCC.

The amounts of added water for the wet granulation are given in Table 2: for the production of MCC 60:40 Ind:Arg 1:1 F only 8.11 % less water was added compared to the production of MCC 80:20 Ind:Arg 1:1 F, whereas the ratio of MCC was reduced by 25.00 %. Therefore, it seems plausible that the MCC 60:40 Ind:Arg 1:1 F batch experienced an overshoot of water that caused an exchange of protons, so salt disproportion and recrystallisation could have taken place. The amount of added water was necessary to reach plastic behaviour and snowball consistency prior to sieving and therefore could not have been reduced according to macroscopic judgement. Another reason for recrystallization could be the demanding production parameters of setting F that lead to heating of the high-shear blender and its content. Higher production temperatures favour recrystallisation since it is defined as a function of temperature, relative humidity, time and/or pressure (Chavan et al., 2016). In can be concluded here that, while the retention of a co-amorphous nature is possible, the choice and combination of formulation and process parameters can influence the outcome.

In Fig. 5 (right) the FTIR spectra of the scaled-up batches are shown after production. The spectra of the batches MCC 80:20 Ind:Arg 1:1 F, MCC 80:20 Ind:Arg 1:1 S and MCC 60:40 Ind:Arg 1:1 S show the typical plateau from 1589 to 1670 cm^{-1} and next to it a sharp drop of absorbance until reaching 1735 cm^{-1}, like the salt-forming lab-scaled batches

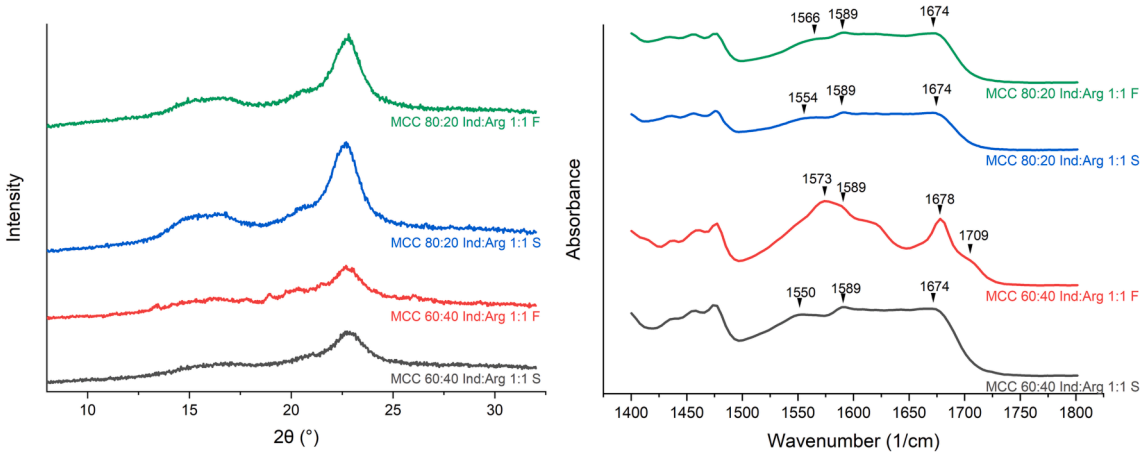

Fig. 5. XRPD (left) and FTIR (right) of the upscaled batches after production. The arrows indicate peaks of each FTIR spectrum that are characteristic for either co-amorphous or crystalline samples.

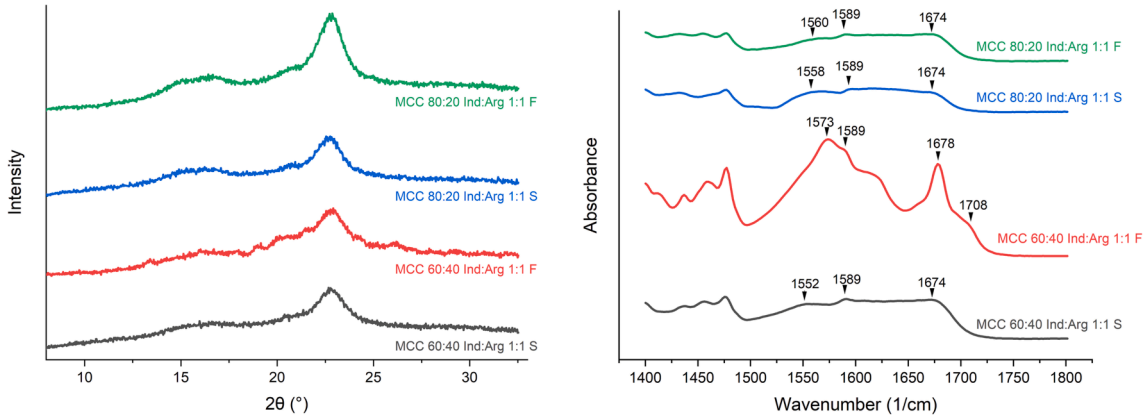

Fig. 6. XRPD (left) and FTIR (right) of the upscaled batches after twelve weeks of storage. The arrows indicate peaks of each FTIR spectrum that are characteristic for either co-amorphous or crystalline samples.

(Fig. 4, right). The absence of any peak around 1700 cm^{-1} and its shift to 1560 cm^{-1} indicates the transduction of a proton from the carboxylic acid moiety of Ind. Salt formation took place in these three batches. The spectrum of MCC 60:40 Ind:Arg 1:1 F (red graph) shows a distinct peak at 1678 cm^{-1} with a downstream shoulder at 1704 cm^{-1} that is caused by the proton still residing at the carboxylic acid moiety of Ind. Furthermore, this spectrum shows its maximum peak at 1574 cm^{-1}, accompanied by a downstream shoulder around 1620 cm^{-1} indicating the presence of the non-ionized form.

Considering the influence of the amount of binder at the harsher process conditions, the composition with the mass ratio of 80 % MCC proved to be more resilient to the demanding mechanical and thermal production parameters, or to be able to compensate an overshoot of added water due to the high water binding capacity of MCC. For both cases it can be concluded that the excipient MCC has a protective effect on the entire granule.

Conclusively, the batches MCC 80:20 Ind:Arg 1:1 F, MCC 80:20 Ind:Arg 1:1 S, MCC 60:40 Ind:Arg 1:1 S were able to undergo wet granulation without recrystallisation whereas batch MCC 60:40 Ind:Arg 1:1 F experienced recrystallisation under the applied production parameters.

3.2.3. *Stability testing of upscaled batches*

The stability of all four upscaled batches was tested via XRPD, DSC and FTIR up to twelve weeks. Comparing the solid state after production

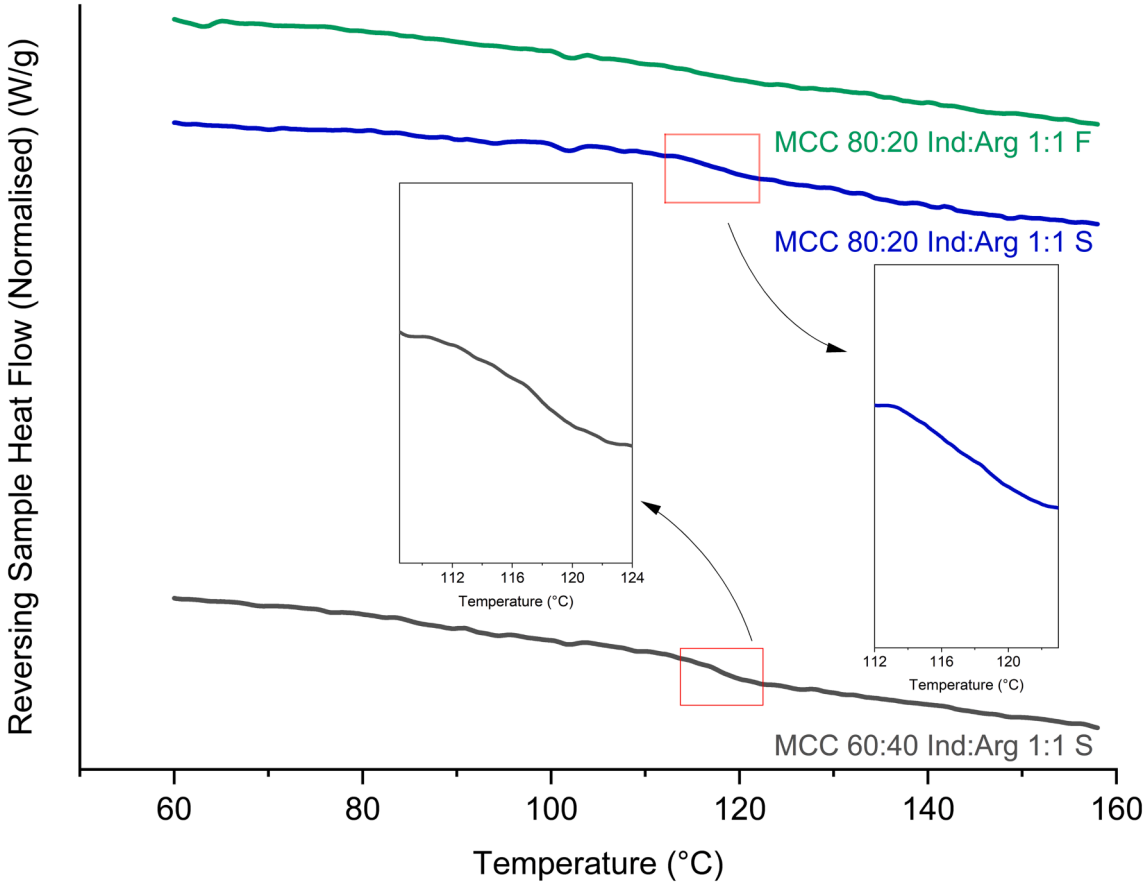

Fig. 7. DSC of the successfully upscaled batches after twelve weeks of storage.

(Fig. 5) with the storage stability results (Fig. 6), no clear differences were observed. This means that the batches that remained co-amorphous upon granulation kept their amorphous nature over the storage period of up to twelve weeks. The system where recrystallization was observed after granulation likewise remained its nature as it showed the respective characteristics after storage. This indicates a stronger impact of the wet granulation process as such on the retention of the amorphous systems, as compared to the storage time.

A similar picture is seen in the FTIR analysis (Fig. 6, right): the initially co-amorphous granules still exhibit a plateau from 1589 to 1670 cm^{-1} followed by a sharp drop of absorbance until reaching 1735 cm^{-1} and a peak shift from 1700 cm^{-1} to 1560 cm^{-1} indicating the conduction of a proton from Ind to Arg and therefore proving the intact salt of these systems. In contrast to this, MCC 60:40 Ind:Arg 1:1 F also has an unchanged spectrum exhibiting the protonated carboxylic acid moiety by its peaks near 1700 cm^{-1} (1678 and 1708 cm^{-1}), proving its unchanged non-salt character (compare Fig. 5).

Thermal analysis of MCC 60:40 Ind:Arg 1:1 S still shows a clear T_g around 118 °C after the full storage period of twelve weeks. In contrast, the DSC diagram of MCC 80:20 Ind:Arg 1:1 F shows no clear T_g after twelve weeks of storage, whereas MCC 80:20 Ind:Arg 1:1 S exhibits a weak step change around 116 °C (Fig. 7). Since neither recrystallisation nor melting events take place in both samples, they can still be assessed as amorphous. The absence of a clear Tg signal may be due to the high ratio of MCC in the system. This might explain the presence of a Tg in the system with a higher amount of amorphous material.

In conclusion three batches could successfully undergo wet granulation under the upscaling settings. The systems remained co-amorphous under retention and presumably due to their intact salt state for the storage period of twelve weeks.

4. Conclusion

In this study, eight different formulations of Ind with two respective co-formers Arg or Trp were investigated and processed via wet granulation with MCC as the sole excipient.

The systems containing Trp had an at least partially crystalline character whereas the Arg containing systems were co-amorphous and maintained this character, as well as their salt structure, for the entire storage time.

For the upscaling attempts of the systems containing Arg, two different mass ratios of MCC to CAMs (80:20 and 60:40) were investigated under two different process conditions, respectively. The applied process conditions showed a stronger influence on recrystallisation than the following storage time. Recrystallisation was associated with the loss of the co-amorphous salt nature and occurred during manufacturing. In general, wet granulation of salt-forming CAMs proved to be feasible.

CRediT authorship contribution statement

David Schütz: Methodology, Formal analysis, Investigation, Writing – original draft, Visualization. **Annika Timmerhaus:** Methodology, Formal analysis, Investigation. **Holger Grohganz:** Conceptualization, Methodology, Writing – review & editing, Supervision, Project administration.

Declaration of Competing Interest

The authors declare that they have no known competing financial interests or personal relationships that could have appeared to influence the work reported in this paper.

Data availability

Data will be made available on request.

Acknowledgments

The authors wish to thank Rikke Helstrup and Kilian Stuhler for providing raw data for one week of stability testing and the sieving analysis of three granule batches, respectively. Chemical structures were created via BIOVIA Draw 2019.

Appendix A. Supplementary material

Supplementary data to this article can be found online at https://doi.org/10.1016/j.ijpharm.2023.123318.

References

Ambrogi, V., Marmottini, F., Pagano, C., 2013. Amorphous carbamazepine stabilization by the mesoporous silicate SBA-15. Microporous Mesoporous Mater. 177, 1–7.
Chavan, R.B., Thipparaboina, R., Kumar, D., Shastri, N.R., 2016. Co amorphous systems: A product development perspective. Int. J. Pharm. 515 (1–2), 403–415.
Cruz-Angeles, J., Videa, M., Martinez, L.M., 2019. Highly Soluble Glimepiride and Irbesartan Co-amorphous Formulation with Potential Application in Combination Therapy. AAPS PharmSciTech 20 (4), 144.
da Costa, N.F., Daniels, R., Fernandes, A.I., Pinto, J.F., 2022a. Amorphous and Co-Amorphous Olanzapine Stability in Formulations Intended for Wet Granulation and Pelletization. Int. J. Mol. Sci. 23 (18), 10234.
da Costa, N.F., Daniels, R., Fernandes, A.I., Pinto, J.F., 2022b. Downstream Processing of Amorphous and Co-Amorphous Olanzapine Powder Blends. Pharmaceutics 14 (8), 1535.
Di, L., Fish, P.V., Mano, T., 2012. Bridging solubility between drug discovery and development. Drug Discov. Today 17 (9–10), 486–495.
Fael, H., Demirel, A.L., 2020. Tannic acid as a co-former in co-amorphous systems: Enhancing their physical stability, solubility and dissolution behavior. Int. J. Pharm. 581, 119284.
Fael, H., Demirel, A.L., 2021. Indomethacin co-amorphous drug-drug systems with improved solubility, supersaturation, dissolution rate and physical stability. Int. J. Pharm. 600, 120448.
Fitch, C.A., Platzer, G., Okon, M., Garcia-Moreno, B.E., McIntosh, L.P., 2015. Arginine: Its pKa value revisited. Protein Sci. 24 (5), 752–761.
Fu, Q., Lu, H.-D., Xie, Y.-F., Liu, J.-Y., Han, Y., Gong, N.-B., Guo, F., 2019. Salt formation of two BCS II drugs (indomethacin and naproxen) with (1R, 2R)-1, 2-diphenylethylenediamine: Crystal structures, solubility and thermodynamics analysis. J. Mol. Struct. 1185, 281–289.
Fung, M.H., DeVault, M., Kuwata, K.T., Suryanarayanan, R., 2018. Drug-Excipient Interactions: Effect on Molecular Mobility and Physical Stability of Ketoconazole-Organic Acid Coamorphous Systems. Mol. Pharm. 15 (3), 1052–1061.
Gershevitz, O., Sukenik, C.N., 2004. In situ FTIR-ATR analysis and titration of carboxylic acid-terminated SAMs. J. Am. Chem. Soc. 126 (2), 482–483.
Grohganz, H., Löbmann, K., Priemel, P., Jensen, K.T., Graeser, K., Strachan, C., Rades, T., 2013. Amorphous drugs and dosage forms. J. Drug Delivery Sci. Technol. 23 (4), 403–408.
Guinet, Y., Paccou, L., Hedoux, A., 2023. Mechanism for Stabilizing an Amorphous Drug Using Amino Acids within Co-Amorphous Blends. Pharmaceutics 15 (2).
Han, J., Wei, Y., Lu, Y., Wang, R., Zhang, J., Gao, Y., Qian, S., 2020. Co-amorphous systems for the delivery of poorly water-soluble drugs: Recent advances and an update. Expert Opin. Drug Deliv. 17 (10), 1411–1435.
Hart, F.D., Boardman, P., 1963. Indomethacin: a new non-steroid anti-inflammatory agent. Br. Med. J. 2 (5363), 965.
Hatwar, P., Pathan, I.B., Chishti, N.A.H., Ambekar, W., 2021. Pellets containing quercetin amino acid co-amorphous mixture for the treatment of pain: Formulation, optimization, in-vitro and in-vivo study. J. Drug Delivery Sci. Technol. 62, 102350.
Hauss, D.J., 2007. Oral lipid-based formulations. Adv. Drug Deliv. Rev. 59 (7), 667–676.
Heikkinen, A., DeClerck, L., Löbmann, K., Grohganz, H., Rades, T., Laitinen, R., 2015. Dissolution properties of co-amorphous drug-amino acid formulations in buffer and biorelevant media. Die Pharmazie-An Int. J. Pharm. Sci. 70 (7), 452–457.
Hoppu, P., Jouppila, K., Rantanen, J., Schantz, S., Juppo, A.M., 2007. Characterisation of blends of paracetamol and citric acid. J. Pharm. Pharmacol. 59 (3), 373–381.
Jensen, K.T., Blaabjerg, L.I., Lenz, E., Bohr, A., Grohganz, H., Kleinebudde, P., Rades, T., Löbmann, K., 2016a. Preparation and characterization of spray-dried co-amorphous drug–amino acid salts. J. Pharm. Pharmacol. 68 (5), 615–624.
Jensen, K.T., Larsen, F.H., Löbmann, K., Rades, T., Grohganz, H., 2016b. Influence of variation in molar ratio on co-amorphous drug-amino acid systems. Eur. J. Pharm. Biopharm. 107, 32–39.
Karagianni, A., Kachrimanis, K., Nikolakakis, I., 2018. Co-Amorphous Solid Dispersions for Solubility and Absorption Improvement of Drugs: Composition, Preparation, Characterization and Formulations for Oral Delivery. Pharmaceutics 10 (3).
Ke, P., Hasegawa, S., Al-Obaidi, H., Buckton, G., 2012. Investigation of preparation methods on surface/bulk structural relaxation and glass fragility of amorphous solid dispersions. Int. J. Pharm. 422 (1–2), 170–178.
Khadka, P., Ro, J., Kim, H., Kim, I., Kim, J.T., Kim, H., Cho, J.M., Yun, G., Lee, J., 2014. Pharmaceutical particle technologies: An approach to improve drug solubility, dissolution and bioavailability. Asian J. Pharm. Sci. 9 (6), 304–316.
Korhonen, O., Pajula, K., Laitinen, R., 2016. Rational excipient selection for co-amorphous formulations. Expert Opin. Drug Deliv. 14 (4), 551–569.

Lenz, E., Jensen, K.T., Blaabjerg, L.I., Knop, K., Grohganz, H., Löbmann, K., Rades, T., Kleinebudde, P., 2015. Solid-state properties and dissolution behaviour of tablets containing co-amorphous indomethacin–arginine. Eur. J. Pharm. Biopharm. 96, 44–52.

Lenz, E., Löbmann, K., Rades, T., Knop, K., Kleinebudde, P., 2017. Hot melt extrusion and spray drying of co-amorphous indomethacin-arginine with polymers. J. Pharm. Sci. 106 (1), 302–312.

Lim, A.W., Löbmann, K., Grohganz, H., Rades, T., Chieng, N., 2016. Investigation of physical properties and stability of indomethacin–cimetidine and naproxen–cimetidine co-amorphous systems prepared by quench cooling, coprecipitation and ball milling. J. Pharm. Pharmacol. 68 (1), 36–45.

Liu, J., Grohganz, H., Löbmann, K., Rades, T., Hempel, N.-J., 2021a. Co-amorphous drug formulations in numbers: Recent advances in co-amorphous drug formulations with focus on co-formability, molar ratio, preparation methods, physical stability, in vitro and in vivo performance, and new formulation strategies. Pharmaceutics 13 (3), 389.

Liu, J., Rades, T., Grohganz, H., 2021b. The influence of moisture on the storage stability of co-amorphous systems. Int. J. Pharm. 605, 120802.

Löbmann, K., Strachan, C., Grohganz, H., Rades, T., Korhonen, O., Laitinen, R., 2012. Co-amorphous simvastatin and glipizide combinations show improved physical stability without evidence of intermolecular interactions. Eur. J. Pharm. Biopharm. 81 (1), 159–169.

Löbmann, K., Grohganz, H., Laitinen, R., Strachan, C., Rades, T., 2013a. Amino acids as co-amorphous stabilizers for poorly water soluble drugs–Part 1: Preparation, stability and dissolution enhancement. Eur. J. Pharm. Biopharm. 85 (3), 873–881.

Löbmann, K., Laitinen, R., Strachan, C., Rades, T., Grohganz, H., 2013b. Amino acids as co-amorphous stabilizers for poorly water-soluble drugs–Part 2: Molecular interactions. Eur. J. Pharm. Biopharm. 85 (3), 882–888.

O'Brien, M., McCauley, J., Cohen, E., 1984. Analytical profiles of drug substances. Indomethacin 13, 211–238.

Ojarinta, R., Heikkinen, A.T., Sievanen, E., Laitinen, R., 2017. Dissolution behavior of co-amorphous amino acid-indomethacin mixtures: The ability of amino acids to stabilize the supersaturated state of indomethacin. Eur. J. Pharm. Biopharm. 112, 85–95.

Ojarinta, R., Saarinen, J., Strachan, C.J., Korhonen, O., Laitinen, R., 2018. Preparation and characterization of multi-component tablets containing co-amorphous salts: Combining multimodal non-linear optical imaging with established analytical methods. Eur. J. Pharm. Biopharm. 132, 112–126.

O'Neil, M.J., 2013. The Merck index: an encyclopedia of chemicals, drugs, and biologicals. RSC Publishing.

Saigal, N., Baboota, S., Ahuja, A., Ali, J., 2009. Microcrystalline cellulose as a versatile excipient in drug research. J. Young Pharm. 1 (1), 6.

Sørensen, C.-M., Rantanen, J., Grohganz, H., 2023. Compaction Behavior of Co-Amorphous Systems. *Pharmaceutics* 15 (3), 858.

Surwase, S.A., Boetker, J.P., Saville, D., Boyd, B.J., Gordon, K.C., Peltonen, L., Strachan, C.J., 2013. Indomethacin: new polymorphs of an old drug. Mol. Pharm. 10 (12), 4472–4480.

Tangirala, A.S., Charithkumar, K., Goswami, T., 2014. Modeling of size reduction, particle size analysis and flow characterisation of spice powders ground in hammer and pin mills. Int. J. Res. Eng. Technol 3, 296–309.

Trasi, N.S., Bhujbal, S., Zhou, Q.T., Taylor, L.S., 2019. Amorphous solid dispersion formation via solvent granulation–A case study with ritonavir and lopinavir. Int. J. Pharm.: X 1, 100035.

Ueda, H., Wu, W., Löbmann, K., Grohganz, H., Müllertz, A., Rades, T., 2018. Application of a salt coformer in a co-amorphous drug system dramatically enhances the glass transition temperature: a case study of the ternary system carbamazepine, citric acid, and l-arginine. Mol. Pharm. 15 (5), 2036–2044.

Vasconcelos, T., Sarmento, B., Costa, P., 2007. Solid dispersions as strategy to improve oral bioavailability of poor water soluble drugs. Drug Discov. Today 12 (23–24), 1068–1075.

Zhang, Y., Gao, Y., Du, X., Guan, R., He, Z., Liu, H., 2020. Combining Co-Amorphous-Based Spray Drying with Inert Carriers to Achieve Improved Bioavailability and Excellent Downstream Manufacturability. Pharmaceutics 12 (11).